DOI: 10.1002/chem.200500285

Simulation of ^{59}Co NMR Chemical Shifts in Aqueous Solution

Michael Bühl,* Sonja Grigoleit, Hendrik Kabrede, and Frank T. Mauschick[a]

Abstract: ^{59}Co chemical shifts were computed at the GIAO-B3LYP level for $[Co(CN)_6]^{3-}$, $[Co(H_2O)_6]^{3+}$, $[Co(NH_3)_6]^{3+}$, and $[Co(CO)_4]^-$ in water. The aqueous solutions were modeled by Car–Parrinello molecular dynamics (CPMD) simulations, or by propagation on a hybrid quantum-mechanical/molecular-mechanical Born–Oppenheimer surface (QM/MM-BOMD). Mean absolute deviations from experiment obtained with these methods are on the order of 400 and 600 ppm, respectively, over a total $\delta(^{59}Co)$ range of about 18000 ppm. The effect of the solvent on $\delta(^{59}Co)$ is mostly indirect, resulting primarily from substantial metal–ligand bond contractions on going from the gas phase to the bulk. The simulated solvent effects on geometries and $\delta(^{59}Co)$ values are well reproduced by using a polarizable continuum model (PCM), based on optimization and perturbational evaluation of quantum-mechanical zero-point corrections.

Keywords: density functional calculations · molecular dynamics · NMR spectroscopy · solvation effects · transition metals

Introduction

NMR chemical shifts obtained from quantum chemistry are known to be "sensitive to everything".[1] For a computational chemist trying to reproduce spectra recorded in typical inert solvents of low polarity, accounting for this surrounding medium is usually not of primary concern, as the choice of quantum-chemical model,[2] basis set,[3] and geometry[4] tend to be much more important for the property under scrutiny. This situation may change for highly polar and/or protic solvents, however, in particular if specific interactions such as hydrogen bonds are involved, as these may have a strong impact on the chemical shifts. In this respect, aqueous solutions are among the most challenging targets. Here, the popular method of including the bulk medium by way of a polarizable continuum[5] in the NMR computation[6] may not be sufficient,[7] and it may be necessary to include discrete solvent molecules or, better yet, a large part of the solution as dynamic ensemble.[8] We have adopted the latter procedure, based on molecular dynamics (MD) simulations in a density functional theory (DFT) framework, to assess chemical shifts of transition-metal nuclei in complexes dissolved in water.[9–12] These nuclei are deemed of special interest because, owing to their large chemical-shift ranges,[13] transition-metal nuclei can be much more sensitive to medium effects than the first-row nuclei.[8]

Indeed, the simulations revealed noticeable changes in magnetic shieldings or chemical shifts of the metal nuclei on immersion in water, albeit to a variable extent: these solvation effects can range from only a few dozen parts per million, as in permanganate ion[11] and most vanadates studied so far,[9,12] to about 2000 ppm for a highly charged ion such as $[Fe(CN)_6]^{4-}$.[10] In the last-named case, this large effect resulted from a pronounced change in geometry on solvation, notably a strong contraction of the metal–ligand bond, and an unusual sensitivity of the ^{57}Fe magnetic shielding toward this geometrical parameter.

Similar effects might be anticipated for the isoelectronic complex $[Co(CN)_6]^{3-}$ (**1**). In the form of its aqueous potassium salt, **1** is the standard for ^{59}Co NMR spectroscopy. This nucleus stands out because of its remarkably large chemical shift range on the order of 20000 ppm.[14] ^{59}Co chemical shifts spanning essentially this entire range have been reproduced reasonably well in computations for isolated molecules and ions, by employing both static[15–17] and dynamic[17] approaches. The latter have been designed to model effects on the δ(metal) values of thermal averaging in the absence of a solvent. In line with recent results for other metal nuclei,[18] these thermal effects can be notable, up to nearly 2000 ppm for $[Co(H_2O)_6]^{3+}$ (**2**),[17] but do not serve to improve the static, equilibrium δ_e values in all cases. Larger deviations have become apparent, in particular for ions such

[a] Dr. M. Bühl, Dr. S. Grigoleit, Dr. H. Kabrede, Dr. F. T. Mauschick
Max-Planck-Institut für Kohlenforschung
Kaiser-Wilhelm-Platz 1, 45470 Mülheim/Ruhr (Germany)
Fax: (+49) 208-306-2996
E-mail: buehl@mpi-muelheim.mpg.de

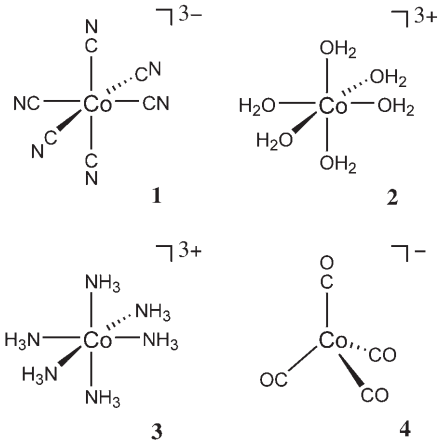

as **2** which were measured in aqueous solution. In addition, a systematic offset of up to about 600 ppm (depending on the particular theoretical level) was noted when the ^{59}Co chemical shifts of a larger test set were referenced directly relative to pristine **1**.[17] These systematic deviations have been ascribed to the aforementioned expected solvent effect on that ion, and an alternative referencing procedure has been adopted, based on the evaluation of the standard magnetic shielding from a correlation of computed shieldings and observed chemical shifts. While this procedure is quite common in cases where the actual standard is difficult or impossible to calculate, its disadvantage is that, in principle, the reference value would have to be re-evaluated for each new complex that is investigated. Eventually, it would be desirable to model substrates and standard in a realistic fashion,[19] so that δ values can be computed and predicted without having to resort to experimental data.

We have now modeled aqueous solutions of **1** and **2** using a variety of methods, namely, molecular dynamics simulations with periodic, fully quantum-mechanical (Car–Parrinello MD) and nonperiodic, mixed quantum-mechanical/molecular mechanical approaches, as well as a polarizable continuum model (PCM).[20] In the last-named calculations, we attempted to go beyond static equilibrium values by inclusion of zero-point vibrational corrections, evaluated by a recent perturbational approach.[21] To our knowledge, this is the first assessment of zero-point effects on chemical shifts in solution.[22]

In addition to the hexaquo complex **2**, which marks the deshielded end of the $\delta(^{59}\mathrm{Co})$ scale, we included the hexammine complex $[Co(NH_3)_6]^{3+}$ (**3**), with a significantly less deshielded nucleus, and the tetracarbonyl ion $[Co(CO)_4]^-$ (**4**), which is close to the shielded end of the $\delta(^{59}\mathrm{Co})$ scale, so that a large part of the total chemical shift range of this nucleus is covered.

Computational Details

Molecular dynamics simulations were performed by using the Car–Parrinello scheme[23] as implemented in the CPMD program.[24] The BP86 combination of density functionals was used,[25,26] together with norm-conserving Troullier–Martins pseudopotentials in the Kleinman–Bylander form,[27] including that for Co constructed and validated in ref. [17]. Periodic boundary conditions were imposed by using cubic supercells with box sizes of 13.0 Å for **1**–**3** and 11.5 Å for **4**, which contained 61 and 45 water molecules, respectively. Kohn–Sham orbitals were expanded in plane waves up to a kinetic energy cutoff of 80 Ry at the Γ point. In the dynamical simulations a fictitious electronic mass of 600 a.u. and a time step of 0.121 fs were used. To increase the simulation time step, hydrogen was substituted by deuterium. The systems were equilibrated for 0.5 ps, maintaining a temperature of 300(±50) K by velocity rescaling, and were then propagated as microcanonical ensemble for an additional 1–2 ps, during which statistical averages and snapshots for the NMR calculations were collected (the latter usually from the first picosecond).

Additional Born–Oppenheimer MD simulations (denoted BOMD) were performed by using the following QM/MM approach: The Co complexes were described at the BP86/AE1 level, that is, with the extended Wachters basis on Co[28] and 6-31G* on the ligands,[29] making use of the resolution-of-identity (RI) approximation as implemented in the TURBOMOLE program,[30] together with suitable auxiliary basis sets.[31] Water was described by the CHARMm force field in the MSI-CHARMm 25b2 program.[32] For the coupling between QM and MM parts, a polarized embedding scheme was used.[33] MD simulations were performed using the ChemShell program[34] for NVT ensembles at 300 K for 4 ps, with a time step of 1 fs. Data sampling was started after the first 2 ps (snapshots from NMR computations after the first 3 ps), which were taken for equilibration. For the aqueous species, the complexes were placed at the center of a spherical water cluster with a diameter of 30 Å containing a total of 453 water molecules. After a short minimization (100 steps), the outmost layer to a depth of 5 Å from the surface was completely frozen to avoid evaporation of the minidroplet. To increase the time step, the O−H distances in the water monomers were frozen with the SHAKE algorithm. For the hexaquo and hexammine complexes, 15 and 16 water molecules, respectively, were included in the QM part; in those cases, no distance constraints were applied within the QM region, and the mass of deuterium was used for all H atoms. Isolated complexes were simulated for 1.5 ps (the first 0.5 ps of which were counted as equilibration) with a time step of 0.5 fs.

PCM calculations were effected at the BP86/AE1 level using the parameters of water and the implementation[35] in Gaussian 03.[36] Zero-point corrections were evaluated following the procedure from reference [21] and the step-size parameters recommended in ref. [37]. Effective (vibrationally averaged) geometries r_{eff} were constructed at the BP86/AE1 level in the continuum, using the gradient technique (i.e., using analytical first derivatives in the numerical evaluation of the cubic force field)[37] and a stepsize of 0.25 a.u.

In all of these static and dynamic calculations the BP86 functional was employed, which performs very well for the description of structures, energies, harmonic frequencies, etc., of transition metal complexes.[38]

Magnetic shieldings σ were computed at the B3LYP level[39,40] for snapshots taken from the MD simulations, employing GIAOs (gauge-including atomic orbitals)[41] and basis II′, that is, the augmented Wachters basis[28] on Co, IGLO-basis[3] II for C, N, O (which is essentially of polarized triple-zeta quality), and IGLO basis DZ for H. This level has been shown to perform very well for chemical shifts of transition metals in general,[42] and ^{59}Co in particular.[17] No periodic boundary conditions were imposed in the chemical-shift calculations. Representative snapshots were taken every 20 fs. Following the procedure from reference [10] a number of nearest solvent water molecules were included explicitly in the NMR calculation (20, 20, 15, and 10 for **1**–**4**, respectively). In all cases, the running averages of σ were reasonably well converged after 1–1.5 ps (40–60 snapshots), with uncertainties of about ±50 ppm for $\sigma(^{59}\mathrm{Co})$, as estimated from the variations in the final values of the running

Table 1. Geometric parameters (mean bond lengths [Å]) and magnetic shielding constants [ppm] for reference compound $[Co(CN)_6]^{3-}$ (**1**).[a]

Level of approximation		r(Co–C)	r(C–N)	σ(Co)
BP86/AE1[b]	$(r,\sigma)_e$	1.929	1.188	−6413
BP86/BOMD	$(r,\sigma)_{av}$	1.939	1.189	−6827
BP86/BOMD/H_2O	$(r,\sigma)_{av}$	1.904	1.186	−5929
BP86/CP-opt[b]	$(r,\sigma)_e$	1.918	1.175	−6025
BP86/CPMD[b]	$(r,\sigma)_{av}$	1.935	1.176	−6680
BP86/CPMD/D_2O	$(r,\sigma)_{av}$	1.895	1.173	−5475
BP86/AE1[b]	$(r,\sigma)_{eff}$	1.937	1.186	−6646
BP86/AE1[b]	σ_0	–	–	−6670
BP86/PCM/AE1[c]	$(r,\sigma)_e$	1.914	1.187	−5977
BP86/PCM/AE1[c]	$(r,\sigma)_{eff}$	1.912	1.182	−5893
BP86/PCM/AE1[c]	σ_0	–	–	−5916
experiment[d]		*1.89(1)*	*1.16(1)*	
		−1.90(1)	*−1.17(1)*	

[a] Geometries evaluated with AE1 or plane-wave basis sets; magnetic shieldings at the GIAO-B3LYP/II′ level; explicit water molecules included for BOMD/H_2O and CPMD/D_2O (see Computational Details). [b] From ref. [17]. [c] FIXGRD,FIXHSS options. [d] Solid $K_3[Co(CN)_6]$, three molecules in the unit cell.[45]

average. Chemical shifts of **2**–**4** are reported relative to **1**, for which the shielding constants are collected in Table 1.

In the perturbational calculation of zero-point corrections, magnetic shieldings were computed at the B3LYP/II′ level for the BP86/PCM-derived effective geometry (denoted σ_{eff}) and vibrationally averaged (denoted σ_0) using numerical evaluation of the second derivative of the shielding surface[21] (stepsize 0.1 a.u.).[37] In addition to the anharmonicity effects contained in the vibrationally averaged effective geometry, this procedure accounts for the curvature of the magnetic shielding hypersurface around the latter. In these computations, the polarizable continuum was also included in the NMR part.

Results and Discussion

$[Co(CN)_6]^{3-}$: CPMD and QM/MM-BOMD simulations were performed for **1**; the latter used the last configuration from the corresponding well-equilibrated run for $[Fe(CN)_6]^{4-}$ as starting point.[10] Before turning to the NMR parameters, we first discuss the structural aspects.

The mean C–N bond length does not vary much and is close to about 1.18–1.19 Å throughout all optimizations and simulations (Table 1). The Co–C distance, in contrast, is more sensitive to dynamics and environment. On going from the equilibrium value to the dynamic average in the gas phase, this distance increases noticeably, by 0.010 Å (compare BP86/AE1 and BOMD entries in Table 1) or by 0.017 Å (compare CP-opt and CPMD). On going from the mean value in the gas phase to that in solution, the bond shrinks considerably, by 0.035 Å (compare BOMD and BOMD/H_2O entries in Table 1) or by 0.040 Å (compare CPMD and CPMD/D_2O). Qualitatively, these are the same structural trends that were found in the related iron species $[Fe(CN)_6]^{4-}$ and $[Fe(CN)_5(NO)]^{2-}$;[10] quantitatively, the effects encountered in **1** are bracketed by those of the latter iron species. For instance, the BOMD-derived M–C bond contraction on hydration is about 0.03, 0.04, and 0.06 Å for $[Fe(CN)_5(NO)]^{2-}$, $[Co(CN)_6]^{3-}$, and $[Fe(CN)_6]^{4-}$, respectively. Thus, the effect increases strongly with increasing molecular charge.

In the case of tetraanionic $[Fe(CN)_6]^{4-}$, earlier periodic CPMD simulations were plagued by artifacts due to the too-small box size (11.5 Å) that could be employed at that time.[10b] The mutual Coulomb repulsion between the anion and its replicated images resulted in a significant additional contraction of the Fe–C bonds by about 0.02 Å, as assessed by the difference between periodic CPMD and nonperiodic BOMD results. Due to the lower charge in tervalent **1**, and further aided by the use of a somewhat larger box (13.0 Å), such artifacts are, apparently, suppressed to a large extent: the CPMD-derived mean Co–O distances are still smaller than the BOMD values, but only by 0.004 Å (BOMD versus CPMD entries in Table 1) or by 0.009 Å (BOMD/H_2O versus CPMD/D_2O entries). While bond-length differences of this magnitude may still translate into noticeable changes in magnetic shieldings (see below), it appears that our CPMD simulations offer a reasonable qualitative and semi-quantitative description of structure and dynamics of aqueous **1**.

As with the iron analogues, the cyano nitrogen atoms in **1** act as hydrogen-bond acceptors from the solvent. Based on purely geometrical criteria,[43] the total number of water molecules H-bonded to **1** varies between 8 and 14, with an average of 11.6. This first solvation shell is also apparent from the $g_{NO}(r)$ pair-correlation function[44] displayed in Figure 1, which shows a distinct maximum at $r = 2.9$ Å ($g = 1.4$).

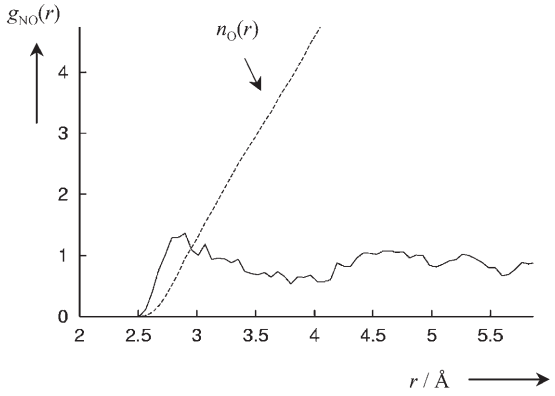

Figure 1. NO pair correlation function $g(r)$ from a CPMD simulation of aqueous **1** (solid line); dashed: $n_O(r) = \rho \int g(r) 4\pi r^2 dr$, which integrates to the total number of oxygen atoms in a sphere with radius r around nitrogen.

The Co–C distances modeled in aqueous solution are close to 1.90 Å, both with BOMD and CPMD variants. Incidentally, this value is close to that typically observed in crystals containing **1**, such as $K_3[Co(CN)_6]$ (see values in Table 1),[45] but also in solids with more bulky counterions and crystal water.[46] Both types of environment, that of an aqueous solution and that of a polar crystal matrix, appear to favor shorter metal–ligand bonds. Packing forces in the

crystal notwithstanding, a possible reason could be that the polar surrounding acts as a dielectric that reduces the intramolecular repulsion between the cyanide ligands with their high negative charge (formally −0.5 e).

Such an effect should already be captured in a simple PCM approach with a polarizable continuum without explicit solvent. Indeed, embedding **1** in such a continuum with the dielectric constant of water by using a molecule-shaped cavity results in a similar contraction of the Co–C bond. With the default settings in Gaussian 03, an optimized distance of 1.902 Å is obtained, in very good accord with the above-mentioned MD-derived values. However, some inconsistencies in the subsequent evaluation of the rovibrational contributions in the continuum were encountered with this setup, namely, conspicuously large gradients in some of the displaced geometries and unrealistically long bonds in the final, effective geometry. No such artifacts were apparent when the geometrical contributions to the first and second derivatives of the electrostatic energy were neglected (i.e., computed at "fixed cavity"). This procedure, which we therefore chose to adopt for **1**, affords an optimized Co–C distance of 1.914 Å (BP86/PCM/AE1 entry in Table 2). Even though this value is slightly larger than that obtained when the forces from the cavity are formally taken into full account, the qualitative result is unaffected by these computational details, namely, that a pronounced bond contraction occurs on solvation. At this point one should recall that despite its wide applicability and success, the PCM approach is based on a very simple model, and the results can also depend on other computational details, notably cavity size. Quantitative accuracy should therefore not be expected, in particular when, as in our case, specific interactions with the solvent molecules are neglected.[47] We therefore consider the numerical PCM data for **1** and the other complexes of this study with a grain of salt, and focus on the qualitative aspects brought about by the simple continuum.

Table 2. Geometric parameters (mean bond lengths [Å]) and ^{59}Co chemical shifts [ppm] for cationic complexes $[CoL_6]^{3+}$ (L = H_2O, NH_3).[a]

Level of approximation		L = H_2O (**2**)		L = NH_3 (**3**)	
		r(Co–O)	$\delta(^{59}Co)$	r(Co–N)	$\delta(^{59}Co)$
BP86/AE1[b]	$(r,\delta)_e$	1.957	15869	2.032	8491
BP86/BOMD	$(r,\delta)_{av}$	1.979	17657	2.069	10132
BP86/BOMD/D_2O	$(r,\delta)_{av}$	1.940	13821	1.995	7184
BP86/CP-opt[b]	$(r,\delta)_e$	1.954	16221	2.019	8265
BP86/CPMD[b]	$(r,\delta)_{av}$	1.975	17747	2.047	8829
BP86/CPMD/D_2O	$(r,\delta)_{av}$	1.952	15723	2.010	8538
BP86/AE1[b]	$(r,\delta)_{eff}$	1.966	16758	2.047	9010
BP86/AE1[b]	δ_0	–	16784	–	9026
BP86/PCM/AE1	$(r,\delta)_e$	1.922	12696	1.982	6760
BP86/PCM/AE1	$(r,\delta)_{eff}$	1.929	14645	2.009	8070
BP86/PCM/AE1	δ_0	–	14655	–	8082
experiment		*1.873(5)*[c]	*15100*[d]	*1.962(6)*	*8176*[f]
				−1.981(7)[e]	

[a] Geometries evaluated with AE1 or plane-wave basis sets; magnetic shieldings at the GIAO-B3LYP/II′ level; explicit water molecules included for BOMD/D_2O and CPMD/D_2O (see Computational Details). [b] From ref. [17]. [c] Solid $CsCo(SO_4)_2 \cdot 12H_2O$, from ref. [58]; see text. [d] Ref. [55]. [e] Ref. [62a]. [f] Ref. [14a].

Zero-point corrections to the structural parameters for **1** in the continuum are quite small; in particular, the Co–C bond length is virtually unaltered (compare BP86/PCM/AE1 r_e and r_{eff} entries in Table 1). The corresponding vibrational corrections in the gas phase lead to a slight elongation of this bond, by 0.008 Å (compare BP86/AE1 r_e and r_{eff} entries in Table 1), qualitatively similar to the classical thermal effect modeled by BOMD and CPMD simulation (see above).[48]

What is the effect of dynamics and solvation on the ^{59}Co magnetic shielding? The computed σ(Co) values in Table 1 exhibit a notable degree of variation, between about −5500 and −6800 ppm, largely following the mean Co–C bond lengths. The longer this bond, the more deshielded is the metal nucleus.[49] Even though they stem from different sources (equilibrium, effective, and ensemble-averaged values with and without solvent or continuum), the r(Co–C) and σ(Co) values from Table 1 show a good linear correlation (correlation coefficient 0.98) with a slope of −285 ppm pm^{-1}, very similar to the corresponding, actual shielding/bond-length derivative in pristine **1**: $\partial\sigma^{Co}/\partial r_{CoC} = -312$ ppm pm^{-1} at the GIAO-B3LYP/II′ level.[17] This result implies that the effect of the solvent on σ(Co) in **1** is mainly indirect, resulting from the change in the geometrical parameters on solvation, a notion which is corroborated by a few explicit test calculations: only minor changes are found for σ(Co) in a CPMD snapshot or in a PCM calculation when the surrounding 20 water molecules or the continuum, respectively, are removed (by 18 and 13 ppm, respectively). Similar observations were made for the iron cyanide complexes mentioned above.[10]

As was noted previously,[16,17] the B3LYP-computed shielding/bond length derivative for **1** is smaller than the experimental estimate for that complex ($\partial\sigma^{Co}/\partial r_{CoC} = -75$ ppm pm^{-1} per bond).[50] The computed value is still quite sizeable, though, and means that any uncertainty in optimized or modeled Co–C distances on the order of 0.01 Å (such as possible artifacts due to box size in the periodic calculations, or due to details of the PCM calculations discussed above) can easily translate into variations in the ^{59}Co magnetic shielding of about 300 ppm. This value should thus be regarded as the lowest error margin for the relative chemical shifts of the other substrates, to which we now turn our attention.

$[Co(H_2O)_6]^{3+}$ (2): At $\delta = 15100$ ppm, this cation marks the deshielded end of the ^{59}Co chemical shift scale.[14,51] Optimizations and simulations of pristine **2** have afforded theoretical chemical shifts exceeding this value by thousands of parts per million.[17] At the same time, this complex was found to be most sensitive to structural changes, with a computed shielding/bond length derivative of $\partial\sigma^{Co}/\partial r_{CoO} = -693$ ppm pm^{-1}.[17] If solvation were to have a similar effect on the geometrical parameters for **2** as it has for **1**, a pro-

nounced effect on the ^{59}Co chemical shift could thus be expected.

When a CPMD simulation was started for **2** in a water box (using the same cell parameter as for **1**, i.e., 13 Å), a surprising observation was made: **2** was not stable under these conditions, but almost instantaneously transferred one proton to the surrounding liquid to afford $[Co(H_2O)_5(OH)]^{2+}$ (**5**) and a hydronium ion H_3O^+. Very rapidly, these two ions dissociated via the well-known proton-relay transport mechanism[52] of aqueous H_3O^+. The same was found in a second simulation when, after 0.9 ps of equilibration with fixed OH bonds, these constraints were lifted; here the first proton transfer occurred after the next 1.4 ps, immediately followed (within 0.1 ps) by relay transfer. These processes were monitored by way of suitable O–H distances and snapshots of the trajectory (Figure 2).

With these results in mind, we set up a QM/MM-BOMD simulation including complex **2** together with 15 additional water molecules from the solvent in the QM part, in order to enable similar proton transfers. However, no such transfers occurred during the total simulation time of 4 ps at the BP86/AE1 level.[53] The reason for this apparent discrepancy between the two simulations, facile or spontaneous proton transfer in CPMD versus no such event in QM/MM-BOMD, is not clear at present. In any event, the occurrence or absence of such a singular event in the rather short simulation times should not be overinterpreted. Much longer simulation times, possibly with inclusion of counterions as well,[54] would be necessary for a definitive assessment. It may also be mandatory to use a larger QM region in the QM/MM calculations to allow for cooperative transport mechanisms as illustrated in Figure 2.

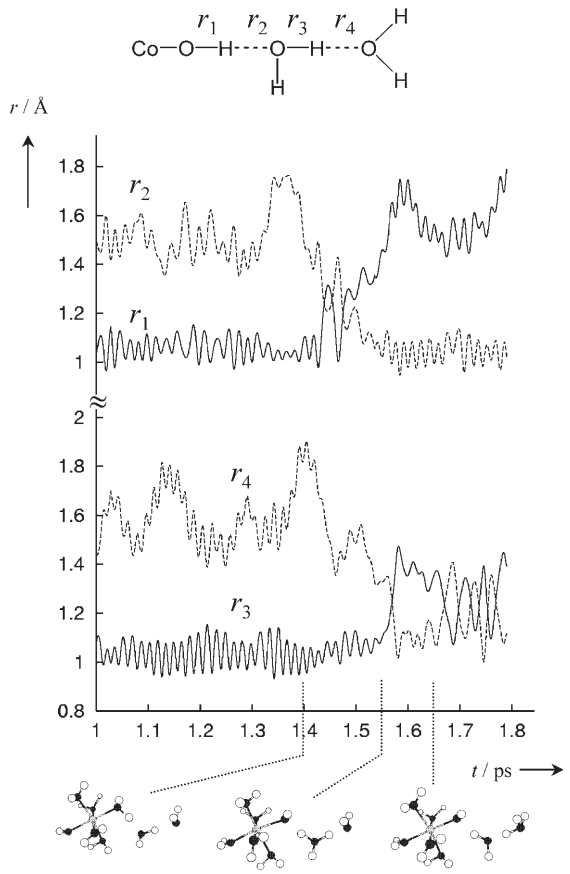

Figure 2. Proton transfers in CPMD simulation of **2** in water (after 0.9 ps of constrained equilibration and 1 ps of unconstrained MD), as followed by the evolution of relevant O–H distances (see top for definition) and illustrative snapshots (bottom, other water molecules omitted).

That deprotonation of **2** may occur in water is not at all improbable, since aqua complexes of high-valent metal cations can be strong Brønsted acids. Indeed, there is evidence for an equilibrium between **2** and **5** from studies of ^{59}Co NMR relaxation times.[55] Owing to the instability of aqueous Co^{3+} solutions, which are rapidly reduced to aqueous Co^{2+}, the pK_a of hydrated Co^{3+}, and thus the composition of the equilibrium mixture between **2** and **5**, is not known. Typical pK_a values of aqueous trivalent transition metal ions fall in the range between about 4 (Cr^{3+}) and 2 (Fe^{3+}).[56] Assuming that the latter value (which is close to that of phosphoric acid) would also apply to Co^{3+}, a degree of dissociation between about 10 and 30% can be anticipated for a pure solution, depending on the total Co concentration (the given percentages correspond to 1 M and 0.1 M, respectively).

The experimental ^{59}Co NMR spectrum, from which the cited δ value was obtained, was recorded in 4 M $HClO_4$ solution.[55] Under these acidic conditions, undissociated **2** will certainly be the principal component of the mixture. We will therefore first evaluate and discuss results from MD trajectories for this species, both from the last 2 ps of the BOMD run and from that part of the CPMD simulation in which the trivalent cation **2** remained intact (taken from 0.4 to 1.4 ps after equilibration in the simulation from Figure 2).

In both cases, each water ligand coordinated to Co donates essentially two hydrogen bonds to the solvent. Since the water ligands are tilted with respect to the Co–O axes, that is, the O atoms appear to coordinate via an sp^3-, rather than an sp^2-type lone pair,[17] they could also accept an additional hydrogen bond from solvent molecules. Such interactions are very rare, however, so that the average number of water molecules coordinated to the hexaquo complex (the second solvation shell around the metal, in other words) is close to 12. This result is also apparent from the $g_{CoO}(r)$ pair-correlation function in Figure 3, which shows a broad, but pronounced peak at $r \approx 4$ Å, with an integrated number of O atoms (up to the next minimum at $r \approx 4.5$ Å) of 11.5 and 11.3 for CPMD and BOMD, respectively.

Up to a distance of $r \approx 4.5$ Å, which marks the approximate boundary between QM and MM regions in the BOMD calculation, the $g_{CoO}(r)$ curves obtained from CPMD and BOMD simulations are remarkably similar, despite the different computational setup (compare black and gray curves in Figure 3). This is especially true for position and shape of the first maximum marking the Co–O distance of the directly coordinated water ligands (cf. the peak positions in the CPMD and BOMD curves) at $r \approx 1.95$–1.96 and 1.94 Å, respectively (the former maximum is somewhat

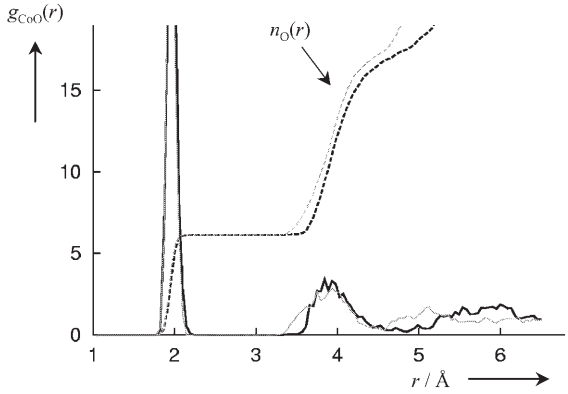

Figure 3. CoO pair correlation function $g(r)$ from CPMD and QM/MM-BOMD simulations (bold and gray lines, respectively) of aqueous **2**; dashed: $n_O(r)$ (see Figure 1 for definition).

broader than the latter), or the actual ensemble averages in Table 2 of $r \approx 1.952$ and 1.941 Å, respectively (see, however, the results for **3** in the next section). Again, both approaches predict a noticeable decrease in the Co–ligand bond length on solvation, namely, by 0.023 and 0.039 Å with CPMD and BOMD, respectively (compare the relevant MD and MD/D_2O data in Table 2). Incidentally, a similar effect is observed in the simple PCM calculations (cf. BP86/AE1 and BP86/PCM/AE1 data), both for equilibrium ($|\Delta r_e| =$ 0.035 Å) and effective geometries ($|\Delta r_{eff}| = 0.037$ Å, Table 2).

All optimizations or simulations including thermal and solvent effects agree that the Co–O distance in aqueous **2** is in the range of about 1.93–1.95 Å. Structural characterization of this highly reactive cation in solution, for instance, by neutron or X-ray scattering studies,[57] is difficult and has not yet been accomplished. Few solids containing tervalent **2** are stable enough to be characterized; the alum-type crystal of $CsCo(SO_4)_2 \cdot 12\,H_2O$, or rather $[Cs(H_2O)_6][Co(H_2O)_6](SO_4)_2$, is a prototypical example.[58] The Co–O distance of 1.873 Å in the latter is significantly shorter than that from our simulations in the aqueous phase. Apparently, the effects of the polar crystal matrix are more pronounced in this case than for anion **1** discussed in the previous section, which is probably related to extensive hydrogen bonding between **2** and the highly charged sulfate anions present in this type of compounds.[59]

How are the computed chemical shifts affected by these geometrical changes? As with **1**, there is a clear correlation between calculated mean Co–O bond lengths and $\delta(^{59}Co)$ values. As the former vary between about 1.92 and 1.98 Å, the latter cover a span of about 13000–18000 ppm (for actual values, see Table 2). The linear regression between the two variables is fair (correlation coefficient 0.96), and the chemical shift/bond length derivative is $+831\ ppm\,pm^{-1}$, a remarkable sensitivity.[60] Best accord with the experimental value is indeed found when both solvent and dynamical effects are accounted for, that is, in the BOMD/D_2O δ_{av}, CPMD/D_2O δ_{av}, and PCM δ_0 (or δ_{eff}) values, with absolute errors from experiment of about 1280, 620, and 450 ppm, respectively. Larger deviations are found for the thermal or zero-point averages in the absence of solvent (e.g., see BOMD and CPMD entries in Table 2). Deceptively good accord with experiment is found for the equilibrium values in the gas phase (see BP86/AE1 and CP-opt data), due to fortuitous error cancellation from the neglect of the mutually opposing dynamic and solvent effects.

In this case, direct solvation effects on ^{59}Co shielding become noticeable: switching off the continuum in the NMR calculation for the PCM-optimized structure results in an additional shielding of the metal nucleus by 262 ppm. A similar shielding effect, up to about 380 ppm, is brought about by deleting the extra solvent molecules in selected MD snapshots. Apparently, the H_2O ligands in **2** are small enough to allow solvent molecules or a continuum to approach the metal center more closely than in **1**, for which negligible direct solvation effects were found (vide supra). In light of the uncertainty in $\delta(^{59}Co)$ arising from the results for the latter standard (see preceding section), however, these direct solvation effects for **2** are barely significant, and the indirect effect via geometrical changes is dominant.

Finally, we evaluated the CPMD results for the deprotonated species in water, that is, for $\mathbf{5}\cdot H_3O^+$ (0–1 ps after equilibration in the first, unconstrained simulation). In this case, the OH ligand in **5** mostly donates one H-bond to the solvent and accepts two others, one of which involves the proton that initially dissociated from **2**. The mean Co–O distance and ^{59}Co chemical shift in the aqueous phase are 1.957 Å and 15635 ppm, respectively, remarkably similar to the corresponding values for intact **2** (cf. CPMD/D_2O values in Table 2). CP optimization and CPMD simulation of pristine **5** in the gas phase also lead to mean Co–O bond lengths (1.951 Å and 1.963 Å, respectively) similar to the corresponding values for free **2** (see CP-opt and CPMD values in Table 2). The reason for this seemingly small geometry change on deprotonation is that the contraction of the hydroxyl C–O bond is compensated by elongation of the Co–O bond to the water ligand in *trans* position (CP-opt parameters are 1.868 and 2.051 Å, respectively). The computed $\delta(^{59}Co)$ resonance in gaseous **5** of 14798 and 15324 ppm at CP-opt and CPMD levels, respectively, is significantly shielded with respect to that of free **2** (see values in Table 2), by up to about 2400 ppm for the CPMD-derived average.[61] It is interesting that in the simulations involving either **2** or **5** in water, this sizeable difference between the two forms essentially vanishes, and their simulated $\delta(^{59}Co)$ values are virtually indistinguishable. Apparently, the strong interaction of the hydroxyl ligand in **5** with the solvent, reflected in the above-mentioned larger number of H-bonding interactions, has a strong impact on the shielding constant of the metal atom. Thus, **2** should display no unusual dependence of $\delta(^{59}Co)$ on pH, in contrast to what would have been predicted from the results in the gas phase.

$[Co(NH_3)_6]$ (3): The number of known cobaltammines is legion, and the parent hexammine complex **3** has been ex-

tensively studied since the days of Alfred Werner. This tervalent cation is part of numerous solids that have been charaterized by X-ray crystallography. Typical Co–N distances are scattered around 1.94–1.98 Å, with longest distances usually found in solids with bulky counterions and crystal water.[62] Again, the simulations in the bulk liquid afford somewhat longer bonds, around 2.00–2.01 Å (Table 2),[63] which are significantly shorter than those simulated in vacuo (ca. 2.05 to 2.07 Å, BOMD/CPMD r_{av} and BP86/AE1 r_{eff} values). Here, we note a minor inconsistency between the QM/MM-BOMD and CPMD simulations: the former predicts a somewhat shorter Co–N distance in the liquid than the latter, by 0.015 Å, and in particular, a much larger bond contraction on solvation, 0.074 Å (BOMD versus BOMD/D_2O values in Table 2), as compared to 0.037 Å (CPMD versus CPMD/D_2O).

From the $g_{CoO}(r)$ pair-correlation function (above $r=3$ Å in Figure 4) it is apparent that the entire second solvation shell is packed more tightly around the complex in the QM/MM-BOMD than in the CPMD trajectory: The first $g_{CoO}(r)$ maximum in the former is shifted somewhat closer to the metal (at $r\approx4$ Å, gray line) than in the latter (at r well above 4 Å, bold line), and, when integrated up to $r=5$ Å, contains a larger number of water molecules (15.7 versus 10.8, respectively).

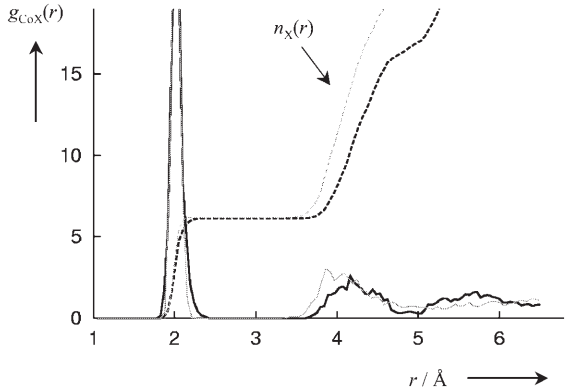

Figure 4. Co(N,O) pair correlation function $g(r)$ from CPMD and QM/MM-BOMD simulations (bold and gray lines, respectively) of aqueous **3**; dashed: $n_{(N,O)}(r)$ (see Figure 1 for definition). The left peaks around 2 Å correspond to $g_{CoN}(r)$, and the curves on the right-hand side to $g_{CoO}(r)$.

Closer inspection of the BOMD trajectory reveals a possible reason for this discrepancy:[64] During the total simulation time of 4 ps, several of the water molecules of the QM region that was initially part of the second solvation shell (i.e., H-bonded to NH_3 ligands), have trailed off into the bulk solvent, to be replaced with a larger number of water molecules from the MM part. Apparently, the latter are bound somewhat tighter to the complex than the former. Similar observations were made in a detailed analysis of the QM/MM-BOMD and CPMD $g_{NO}(r)$ functions of aqueous $[Fe(CN)_6]^{4-}$.[10b] In the QM/MM-BOMD simulation for **2**, in contrast, the water molecules are bound more strongly to the complex from the beginning, so that the molecules of the QM region remain in a closer sphere around the solute during the limited simulation time, without significant penetration of "MM water" into this second solvation shell. It is possible that in this simulation, if continued long enough, exchange between water molecules from the second solvation sphere and the bulk liquid will take place eventually, and that the structures of the water shell around **2**, as they emerge from QM/MM-BOMD and CPMD simulations (Figure 3), will become more disparate. A circumvention of this problem could be to increase the QM part, or to assign QM and MM regions not to specific atoms throughout, but to predefined regions in space, by employing suitable smoothing functions that allow for continuous transition of molecules from one region to the other.[65,66] Clearly, further theoretical work in that direction is warranted.[67] With these artifacts of the present QM/MM-BOMD simulation in mind, we now turn to the ^{59}Co chemical shift of **3**.

As with the results for **2** discussed above, the metal–ligand distance strongly affects the $\delta(^{59}Co)$ value of **3**. Since the Co–X shielding/bond length derivative in pristine **3** of -471 ppm pm^{-1},[17,68] is smaller than that in **2**, the sensitivity of $\delta(^{59}Co)$ in **3** is somewhat less pronounced than in the hexaquo complex, but with $\delta\approx7000$–10 000 ppm the variations are still sizeable. Apart from the fortuitously good accuracy of the BP86/AE1 and CP-opt equilibrium δ_e data, best accord with experiment is found for the CPMD/D_2O (δ_{av}) and BP86/PCM values (δ_{eff} or δ_0, Table 2). In line with the preceding discussion of the solvation shell derived from the QM/MM-BOMD simulations in water, the ^{59}Co chemical shift is significantly underestimated by this model, and falls short of experiment by almost 1000 ppm (see BOMD/D_2O entry in Table 2). Apparently, the extent of the bond contraction in solution, that is, the indirect solvation effect, is overestimated in our simulation, probably by some 0.01–0.02 Å.

In addition to the relative sensitivity of the ^{59}Co shielding in **2** and **3** toward the geometrical parameters,[17] the direct solvation effect on this property decreases somewhat on going from **2** to **3**. For instance, omitting the continuum in the NMR calculation for the BP86/PCM optimized structure of **3** affords an additional shielding of the metal by 176 ppm. The differential effect between the CPMD and QM/MM-BOMD results due to the more compact second solvation shell in the latter simulation should be even smaller. Thus, it is the averaged parameters of the metal complex itself that are decisive for the computed ^{59}Co chemical shift of aqueous **3**. The ability to reproduce both is thus a stringent test for QM/MM methods.

Finally, we mention an additional potential source of deviations between the experimental value given in Table 2 and some of the computed $\delta(^{59}Co)$ data: In the CPMD simulations (as well as in the QM/MM-BOMD runs), H atoms were substituted by deuterium to improve the stability of the simulation in terms of energy conservation in the chosen time step. Thus, these computations are actually modeling $[Co(ND_3)_6]^{3+}$ ($[D_{18}]$-**3**), for which a noticeable isotope effect

was noted experimentally: the observed upfield shift of 5.2–5.6 ppm per H/D substitution in **3**[69] amounts to a total isotope effect of $\Delta\delta(^{59}\mathrm{Co}) \approx -100$ ppm for the fully deuterated complex.[70] We have evaluated this secondary isotope effect for **3**, employing the (mass-dependent) perturbational zero-point corrections in the gas phase. With this method, even more subtle H/D isotope effects in cobaloximes[71] have been reproduced and interpreted computationally.[17] On going from **3** to [D_{18}]-**3**, a shielding of the ^{59}Co resonance of −105 ppm is computed, in excellent agreement with experiment. This increase in shielding can be traced back to a slight contraction of the Co–N bond (by 0.002 Å) on deuteration. It is gratifying that such relative trends between isotopomers can be fairly well modeled computationally. However, as far as $\delta(^{59}\mathrm{Co})$ values between the different species of this study are concerned, such isotope effects are well below the uncertainty of 300 ppm estimated from the results for the standard **1** (see above).

$[Co(CO)_4]^-$ (4): To test the performance of the methods applied so far in cases where much smaller solvation effects are to be expected, we included the tetracarbonylate complex **4** in this study. Owing to the more hydrophobic nature of its ligands and its overall smaller charge, the interaction with a polar solvent and thus the effect of the latter on the ^{59}Co magnetic shielding constant should be much less pronounced in this case. This was specifically tested for two approaches: a CPMD simulation in water and PCM computations. The results are summarized in Table 3.

Table 3. Geometric parameters (mean bond lengths [Å]) and ^{59}Co chemical shifts [ppm] for $[Co(CO)_4]^-$ (**4**).[a]

Level of approximation		r(Co–C)	$\delta(^{59}\mathrm{Co})$
BP86/AE1[b]	$(r,\delta)_e$	1.777	−3493
BP86/CP-opt[b]	$(r,\delta)_e$	1.771	−3196
BP86/CPMD[b]	$(r,\delta)_{av}$	1.777	−3721
BP86/CPMD/D_2O	$(r,\delta)_{av}$	1.769	−2594
BP86/AE1[b]	$(r,\delta)_{eff}$	1.782	−3667
BP86/AE1[b]	δ_0	–	−3680
BP86/PCM/AE1	$(r,\delta)_e$	1.770	−3118
BP86/PCM/AE1	$(r,\delta)_{eff}$	1.782	−2985
BP86/PCM/AE1	δ_0	–	−2995
experiment		*1.754(5)*	*−3100*[d]
		−1.764(5)[c]	

[a] Geometries evaluated with AE1 or plane-wave basis sets; magnetic shieldings at the GIAO-B3LYP/II′ level; explicit water molecules included for CPMD/D_2O (see Computational Details). [b] From ref. [17]. [c] Solid, from ref. [72a]. [d] Na^+ salt in water, from ref. [14a].

This ion is frequently encountered in organocobalt chemistry and has been structurally characterized in dozens of single crystals, albeit in none containing additional water molecules, the solvent used in the NMR experiments. Most Co–C distances fall into the range between about 1.74 and 1.77 Å, with larger values typically observed in low-temperature structures containing bulky counterions and cocrystallized organic solvent molecules.[72] Slightly larger distances, between about 1.77 and 1.78 Å are obtained from optimizations or simulations (Table 3). As expected, relatively small solvation effects on this parameter are indicated by CPMD and PCM calculations, which afford slight bond contractions of less than 0.01 Å (compare CPMD versus CPMD/D_2O and BP86/AE1 versus BP86/PCM/AE1 entries).

In the CPMD simulation in water, little specific interaction between solvent and solute is apparent. Occasionally, O–H bonds of the former point toward carbonyl O atoms of the latter such that the formal geometrical criteria[43] for an O···H–O hydrogen bond are fulfilled. Such contacts are sparse and short-lived, however, and on average the number of such potential H-bonded water molecules around **4** is only about 2. The lack of such specific interactions is also reflected in the O(carbonyl)/O(water) pair-correlation function displayed in Figure 5, which shows no pronounced maximum up to $r = 3.5$ Å,[73] in contrast to the corresponding $g_{NO}(r)$ curve in trianionic **1**, which has a distinct peak at $r \approx 2.8$ Å (Figure 1).

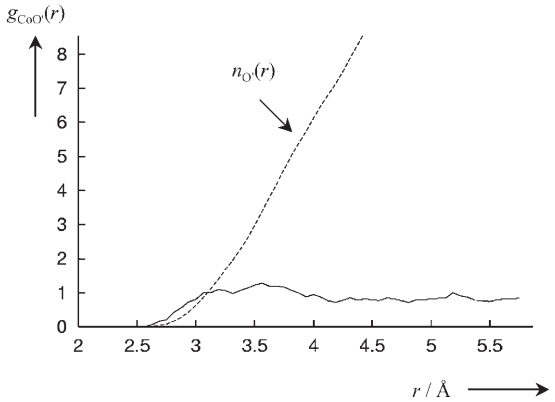

Figure 5. O(carbonyl)/O′(water) pair correlation function $g(r)$ from a CPMD simulation of aqueous **4** (solid line); dashed: total number of water oxygen atoms in a sphere of radius r around the carbonyl O atoms.

Consistent with these weak solvent–solute interactions, the small geometrical changes on solvation, and the comparatively small sensitivity toward the Co–C bond length (shielding/bond length derivative -132 ppm pm^{-1}),[17] we find only minor variations in the ^{59}Co shielding constant, barely exceeding 100 ppm, with the different approaches. The large fluctuations of $\delta(^{59}\mathrm{Co})$ apparent in Table 3 are a consequence of the changes in σ of the standard **1** with the computational model (see Table 1). The large deshielding of the metal nucleus in **1** when thermal or zero-point corrections are included in the gas phase only leads to a noticeable upfield shift of the corresponding $\delta(^{59}\mathrm{Co})$ resonances of **4** relative to this standard, by up to about 500–600 ppm (see CPMD δ_{av} and BP86/AE1 δ_{eff} and δ_0 values in Table 3). In contrast, a downfield shift of $\delta(^{59}\mathrm{Co})$ by about the same amount is found from the CPMD/D_2O simulations. In this case it is just the PCM approaches that afford ^{59}Co chemical shifts well within 300 ppm of experiment.

Final Assessment and Conclusion

How well do the various approaches employed here perform in the computation of the ^{59}Co chemical shifts of **1**–**4**? Qualitatively, the correct sequence and orders of magnitude are reproduced by all of the DFT methods applied. The factors that govern these qualitative aspects are well understood, and ^{59}Co chemical shifts can be successfully interpreted in terms of simple ligand-field parameters.[74] In a quantum-mechanical picture, the ordering and spacing of chemical shifts is usually governed by the paramagnetic part of the shielding constant, arising from the magnetic coupling of suitable occupied and unoccupied MOs.[75,76] The key requirements for the presence of large paramagnetic contributions are proper symmetries of such MO pairs that contain large contributions from the nucleus under scrutiny, and small energetic separations between these MOs.

Compared to these underlying characteristics of the electronic structure, the thermal and solvation effects which are the target of this study are more subtle and more difficult to analyze. We limit ourselves to a comparative assessment of the various methods employed, gauging their merits in the ability to reproduce the $\delta(^{59}\mathrm{Co})$ values of **1**–**4** as accurately as possible. A summary of results from linear regressions of the experimental ^{59}Co chemical shifts versus those computed with the various approaches is collected in Table 4 and, for some illustrative levels, displayed in Figure 6.

We are aware that a set of just four compounds is too small to obtain statistically meaningful results. However, the data in Table 4 and the plots in Figure 6 nicely illustrate some of the recurring themes from the preceding discussions of the individual species. As was noted for a larger test set of Co complexes,[17] static gas-phase equilibrium values are in fortuitously good accord with experiment (note the small mean errors and near-ideal slopes for BP86/AE1 and CP-opt results in Table 4 and Figure 6). This accord deteriorates when thermal or zero-point corrections are added to these gas-phase data, as evidenced by the resulting larger mean errors and slopes (e.g., compare CP-opt and CPMD in Table 4 and Figure 6). Immersion in water reduces both errors and slopes and restores an excellent agreement with experiment for the CPMD/D_2O data, whereas a tendency toward overcorrection of the solvent effect is apparent from the QM/MM-BOMD/D_2O results (note in particular the corresponding slope in Table 4 of 0.91, which is significantly smaller than unity). At least in one case, namely, **3**, a problem with our particular QM/MM partition of the bulk solvent was identified as possible source of this deviation. This caveat notwithstanding, the mean error in $\delta(^{59}\mathrm{Co})$ obtained with this approach of about 600 ppm (Table 4), is still acceptable when compared to the total shift range covered of

Table 4. Statistical analysis from linear regression of calculated versus experimental ^{59}Co chemical shifts of **1**–**4**.

Level of approximation		MAE[a]	Slope	Intercept
BP86/AE1	δ_e	369	1.06	−124
BP86/BOMD[b]	δ_{av}	1504	1.17	174
BP86/BOMD/D_2O[b]	δ_{av}	609	0.91	−91
BP86/CP-opt	δ_e	327	1.06	−28
BP86/CPMD	δ_{av}	979	1.17	−169
BP86/CPMD/D_2O	δ_{av}	373	1.02	291
BP86/AE1	δ_{eff}	765	1.12	−113
BP86/AE1	δ_0	779	1.12	−117
BP86/PCM/AE1	δ_e	960	0.86	−251
BP86/PCM/AE1	δ_{eff}	169	0.97	34
BP86/PCM/AE1	δ_0	161	0.97	31

[a] Mean absolute error in ppm. [b] For **1**–**3**.

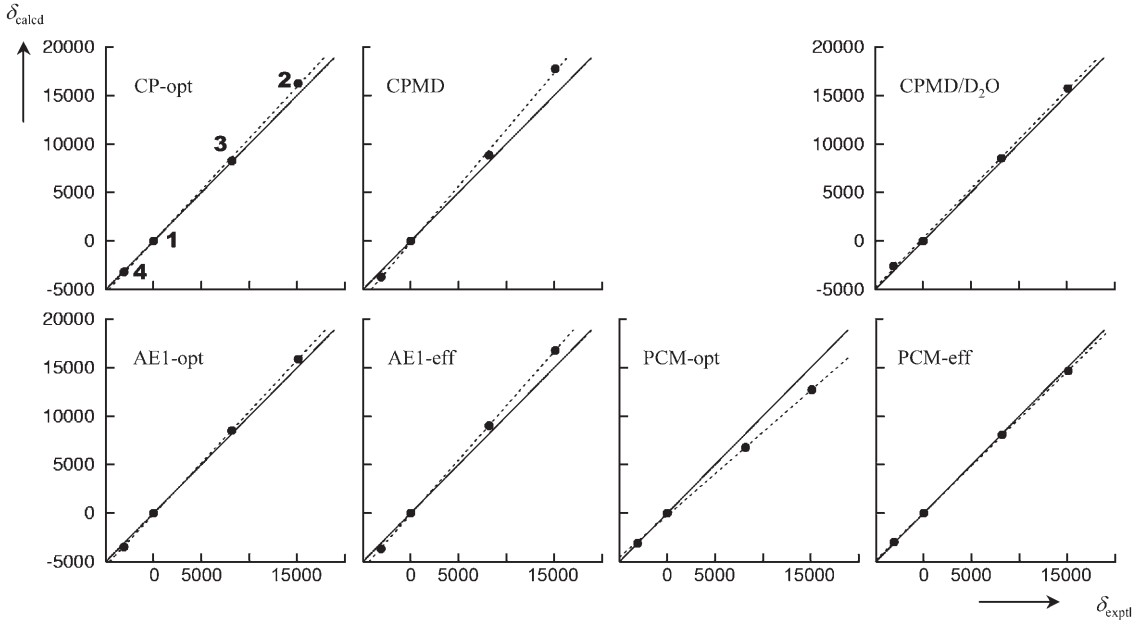

Figure 6. Plot of calculated versus experimental ^{59}Co chemical shifts of **1**–**4** for selected theoretical levels (opt, MD, and eff denote δ_e, δ_{av}, and δ_{eff} values, respectively). Solid lines: ideal slope 1, dashed: linear fit.

18 000 ppm (3%). On such a relative basis, the accuracy achieved with the CPMD/D_2O approach, with a mean error of about 400 ppm or 2% of the shift range, can be considered excellent.

The principal effect of the solvent is contraction of the cobalt–ligand bonds and concomitant shielding of the metal nucleus. Both are qualitatively captured in a simple standard PCM approach. While static optimizations in the continuum tend to overestimate such solvation effects (e.g., note the smaller slope of the PCM-opt plot in Figure 6), a combination of PCM and vibrational zero-point corrections (which we present for the first time) appears to perform very well. Incidentally, this combined method affords the best results for the systems of this study, as judged from the very small deviations from experiment (see PCM δ_{eff} and δ_0 data in Table 4, and the PCM-eff plot in Figure 6). As noted above, however, this finding should not be overrated, but should rather invite further systematic tests of how the PCM results depend on other computational details such as effects of cavity size or finite temperature.

Almost all of the computed total zero-point correction to $\delta(^{59}Co)$ is contained in the value at the effective, vibrationally averaged geometry (δ_{eff}), both in vacuo (as found for all transition-metal nuclei so far[17,18,77]) and in the continuum. The additional modulations from the curvature of the magnetic shielding surface around the effective geometry are so small that they can be safely neglected (note the very small differences between δ_{eff} and δ_0 values in Tables 2–4).

In summary, ^{59}Co chemical shifts of a small set of inorganic and organometallic cobalt complexes in aqueous solution can be well reproduced computationally, provided that effects of both vibrational averaging and solvation are taken explicitly or implicitly into account. A number of practical methods to achieve this have been successfully tested. Among these, the approach based on CPMD simulations of the actual solution performs particularly well. A combination of zero-point corrections and a simple polarizable continuum also appears to hold some promise.

The complexes of this study, small and highly charged ions with an exceptionally sensitive NMR nucleus, are probably among the most challenging targets for this kind of property computation. The available theoretical tools for treating thermal and solvent effects on chemical shifts have been shown to pass this stringent test, thereby further establishing their potential usefulness in NMR calculations of transition-metal complexes. This small test set of cobalt complexes appears to be very well suited to assess newly developed or refined methods and density functionals for such property calculations.

Acknowledgements

M.B. wishes to thank Prof. W. Thiel, the MPI Mülheim, and the Deutsche Forschungsgemeinschaft for support. Computations were performed on Compaq XP1000 and ES40 workstations as well as on an Intel Xeon PC cluster at the MPI Mülheim, and on an IBM p690 "Regatta" cluster at the Rechenzentrum Garching of the Max Planck Society.

[1] G. Schreckenbach, S. K. Wolff, T. Ziegler, *J. Phys. Chem. A* **2000**, *104*, 8244–8255.
[2] See, for instance: a) T. Helgaker, M. Jaszunski, K. Ruud, *Chem. Rev.* **1999**, *99*, 293–352; b) M. Bühl, M. Kaupp, V. G. Malkin, O. L. Malkina, *J. Comput. Chem.* **1999**, *20*, 91–105; c) *Calculation of NMR and ESR Parameters. Theory and Applications* (Eds.: M. Kaupp, M. Bühl, V. G. Malkin), Wiley-VCH, Weinheim, **2004**.
[3] W. Kutzelnigg, U. Fleischer, M. Schindler in *NMR Basic Principles and Progress, Vol. 23*, Springer, Berlin, **1990**, pp. 165–262.
[4] See, for instance: M. Bühl in *Encyclopedia of Computational Chemistry* (Eds.: P. von R. Schleyer, N. L. Allinger, P. A. Kollman, T. Clark, H. F. Schaefer, J. Gasteiger, P. R. Schreiner), Wiley, Chichester, **1998**, pp. 1835–1845.
[5] J. Tomasi, M. Persico, *Chem. Rev.* **1994**, *94*, 2027–2094.
[6] I. Ciofini in *Calculation of NMR and ESR Parameters. Theory and Applications*, (Eds.: M. Kaupp, M. Bühl, V. G. Malkin), Wiley-VCH, Weinheim, **2004**, pp. 191–208.
[7] An example for the description of the chemical shifts of liquid water: R. A. Klein, B. Mennuci, J. Tomasi, *J. Phys. Chem. A* **2004**, *108*, 5851–5863.
[8] a) V. G. Malkin, O. L. Malkina, G. Steinebrunner, H. Huber, *Chem. Eur. J.* **1996**, *2*, 452–457; b) B. G. Pfrommer, F. Mauri, S. G. Louie, *J. Am. Chem. Soc.* **2000**, *122*, 123–129; c) D. Sebastiani, M. Parrinello, *J. Phys. Chem. A* **2001**, *105*, 1951–1958; d) D. J. Searles, H. Huber in *Calculation of NMR and ESR Parameters. Theory and Applications*, (Eds.: M. Kaupp, M. Bühl, V. G. Malkin), Wiley-VCH, Weinheim, **2004**, pp. 175–189.
[9] M. Bühl, M. Parrinello, *Chem. Eur. J.* **2001**, *7*, 4487–4494.
[10] a) M. Bühl, F. T. Mauschick, F. Terstegen, B. Wrackmeyer, *Angew. Chem.* **2002**, *114*, 2417–2420; *Angew. Chem. Int. Ed.* **2002**, *41*, 2312–2315; b) M. Bühl, F. T. Mauschick, *Phys. Chem. Chem. Phys.* **2002**, *4*, 5508–5514.
[11] M. Bühl, *J. Phys. Chem. A* **2002**, *106*, 10505–10509.
[12] M. Bühl, R. Schurhammer, P. Imhof, *J. Am. Chem. Soc.* **2004**, *126*, 3310–3320.
[13] *Transition Metal Nuclear Magnetic Resonance* (Ed.: P. S. Pregosin), Elsevier, Amsterdam, **1991**.
[14] a) P. S. Pregosin in *Transition Metal Nuclear Magnetic Resonance* (Ed.: P. S. Pregosin), Elsevier, Amsterdam, **1991**, p. 144–215; b) A. Yamasaki, *J. Coord. Chem.* **1991**, *24*, 211–260; c) J. C. C. Chan, S. C. F. Au-Yeung, *Annu. Rep. NMR Spectrosc.* **2000**, *41*, 1–54.
[15] a) J. C. C. Chan, S. C. F. Au-Yeung, P. J. Wilson, G. A. Webb, *J. Mol. Struct.* **1996**, *365*, 125–130; b) J. C. C. Chan, S. C. F. Au-Yeung, *J. Mol. Struct.* **1997**, *393*, 93–96; c) J. C. C. Chan, S. C. F. Au-Yeung, *J. Phys. Chem. A* **1997**, *101*, 3637–3640.
[16] N. Godbout, E. Oldfield, *J. Am. Chem. Soc.* **1997**, *119*, 8065–8069.
[17] S. Grigoleit, M. Bühl, *J. Chem. Theory Comput.* **2005**, *1*, 181–193.
[18] S. Grigoleit, M. Bühl, *Chem. Eur. J.* **2004**, *10*, 5541–5552.
[19] Computing highly charged anions such as **1** in the gas phase is unrealistic in the sense that the expected spontaneous electron detachment is only prevented by the finite basis set (or, in the periodic plane-wave calculations, by a compensating, smeared-out background charge).
[20] a) V. Barone, M. Cossi, J. Tomasi, *J. Comput. Chem.* **1998**, *19*, 404–417; b) M. Cossi, G. Scalmani, N. Rega, V. Barone, *J. Chem. Phys.* **2002**, *117*, 43–54; c) M. Cossi, O. Crescenzi, *J. Chem. Phys.* **2003**, *119*, 8863–8872.
[21] a) K. Ruud, P.-O. Åstrand, P. R. Taylor, *J. Chem. Phys.* **2000**, *112*, 2668–2683; b) K. Ruud, P.-O. Åstrand, P. R. Taylor, *J. Am. Chem. Soc.* **2001**, *123*, 4826–4833; c) T. Ruden O. B. Lutnæes, T. Helgaker, K. Ruud, *J. Chem. Phys.* **2003**, *118*, 9572–9581.
[22] Rovibrational effects on the magnetic shielding constants in TcO_4^- were recently evaluated in a polarizable continuum: H. Cho, W. A. de Jong, B. K. McNamara, B. M. Rapko, I. E. Burgeson, *J. Am. Chem. Soc.* **2004**, *126*, 11583–11588.
[23] R. Car, M. Parrinello, *Phys. Rev. Lett.* **1985**, *55*, 2471–2474.
[24] CPMD Version 3.7.0, copyright by IBM Corp. and Max-Planck-Institut für Festkörperforschung, Stuttgart, Germany.

[25] A. D. Becke, *Phys. Rev. A* **1988**, *38*, 3098–3100.
[26] a) J. P. Perdew, *Phys. Rev. B* **1986**, *33*, 8822–8824; b) J. P. Perdew, *Phys. Rev. B* **1986**,*34*, 7406.
[27] a) N. Troullier, J. L. Martins, *Phys. Rev. B* **1991**, *43*, 1993–2006; b) L. Kleinman, D. M. Bylander, *Phys. Rev. Lett.* **1982**, *48*, 1425–1428.
[28] a) A. J. H. Wachters, *J. Chem. Phys.* **1970**, *52*, 1033–1036; b) P. J. Hay, *J. Chem. Phys.* **1977**, *66*, 4377–4384.
[29] a) W. J. Hehre, R. Ditchfield, J. A. Pople, *J. Chem. Phys.* **1972**, *56*, 2257–2261; b) P. C. Hariharan, J. A. Pople, *Theor. Chim. Acta.* **1973**, *28*, 213–222.
[30] R. Ahlrichs, M. Bär, M. Häser, H. Korn, M. Kölmel, *Chem. Phys. Lett.* **1989**, *154*, 165–169.
[31] a) K. Eichkorn, O. Treutler, H. Öhm, M. Häser, R. Ahlrichs, *Chem. Phys. Lett.* **1995**, *240*, 283–289; b) K. Eichkorn, O. Treutler, H. Öhm, M. Häser, R. Ahlrichs, *Chem. Phys. Lett.* **1995**, *242*, 652–660;c) K. Eichkorn, F. Weigend, O. Treutler, R. Ahlrichs, *Theor. Chem. Acc.* **1997**, *97*, 119–124.
[32] QUANTA98, Molecular Simulations, Inc., 9685 Scranton Rd. San Diegom CA 92121. The published results were generated using the program CHARMm. This program is distributed by Molecular Simulations Inc.
[33] Corresponding to model B in D. Bakowies, W. Thiel, *J. Phys. Chem.* **1996**, *100*, 10580–10594.
[34] a) P. Sherwood, A. H. deVries, ChemShell—A Shell for Computational Chemistry, CCLRC Daresbury Laboratory, **1999**; see http://www.dl.ac.uk; b) P. Sherwood, A. de Vries, M. Guest, G. Schreckenbach, R. Catlow, S. French, A. Sokol, S. Bromley, W. Thiel, A. Turner, S. Billeter, F. Terstegen, S. Thiel, J. Kendrick, S. Rogers, J. Casci, M. Watson, F. King, E. Karlsen, M. Sjovoll, A. Fahmi, A. Schäfer, C. Lennartz, *J. Mol. Struct.* **2003**, *632*, 1–28.
[35] a) S. Miertus, E. Scrocco, J. Tomasi, *Chem. Phys.* **1981**, *55*, 117–129; b) B. Mennucci, J. Tomasi, *J. Chem. Phys.* **1997**, *106*, 5151–5158; c) V. Barone, M. Cossi, J. Tomasi, *J. Chem. Phys.* **1997**, *107*, 3210–3221.
[36] Gaussian 03, Revision B01, M. J. Frisch, G. W. Trucks, H. B. Schlegel, G. E. Scuseria, M. A. Robb, J. R. Cheeseman, J. A. Montgomery, Jr., T. Vreven, K. N. Kudin, J. C. Burant, J. M. Millam, S. S. Iyengar, J. Tomasi, V. Barone, B. Mennucci, M. Cossi, G. Scalmani, N. Rega, G. A. Petersson, H. Nakatsuji, M. Hada, M. Ehara, K. Toyota, R. Fukuda, J. Hasegawa, M. Ishida, T. Nakajima, Y. Honda, O. Kitao, H. Nakai, M. Klene, X. Li, J. E. Knox, H. P. Hratchian, J. B. Cross, C. Adamo, J. Jaramillo, R. Gomperts, R. E. Stratmann, O. Yazyev, A. J. Austin, R. Cammi, C. Pomelli, J. W. Ochterski, P. Y. Ayala, K. Morokuma, G. A. Voth, P. Salvador, J. J. Dannenberg, V. G. Zakrzewski, S. Dapprich, A. D. Daniels, M. C. Strain, O. Farkas, D. K. Malick, A. D. Rabuck, K. Raghavachari, J. B. Foresman, J. V. Ortiz, Q. Cui, A. G. Baboul, S. Clifford, J. Cioslowski, B. B. Stefanov, G. Liu, A. Liashenko, P. Piskorz, I. Komaromi, R. L. Martin, D. J. Fox, T. Keith, M. A. Al-Laham, C. Y. Peng, A. Nanayakkara, M. Challacombe, P. M. W. Gill, B. Johnson, W. Chen, M. W. Wong, C. Gonzalez, J. A. Pople, Gaussian, Inc., Pittsburgh, PA, **2003**.
[37] M. Bühl, P. Imhof, M. Repisky, *ChemPhysChem* **2004**, *5*, 414–418.
[38] See, for instance: a) W. Koch, M. C. Holthausen, *A Chemist's Guide to Density Functional Theory*, Wiley-VCH, Weinheim, **2000**, and the extensive bibliography therein; b) see also the special issue of *Chem. Rev.* **2000**, *100*, 351–818 on Computational Transition Metal Chemistry.
[39] C. Lee, W. Yang, R. G. Parr, *Phys. Rev. B* **1988**, *37*, 785–789.
[40] A. D. Becke, *J. Chem. Phys.* **1993**, *98*, 5648–5652.
[41] a) R. Ditchfield, *Mol. Phys.* **1974**, *27*, 789–807; b) K. Wolinski, J. F. Hinton, P. Pulay, *J. Am. Chem. Soc.* **1990**, *112*, 8251–8260; GIAO-DFT implementation: c) J. R. Cheeseman, G. W. Trucks, T. A. Keith, M. J. Frisch, *J. Chem. Phys.* **1996**, *104*, 5497–5509.
[42] a) M. Bühl, *Chem. Phys. Lett.* **1997**, *267*, 251–257; b) M. Bühl in *Calculation of NMR and ESR Parameters. Theory and Applications*, (Eds.: M. Kaupp, M. Bühl, V. G. Malkin), Wiley-VCH, Weinheim, **2004**, pp. 421–431.
[43] A hydrogen bond is assigned if the O···X distance is smaller than 3.5 Å and the O–H bond is directed towards the heteroatom such that the O–H···X angle is larger than 140°; cf. the corresponding criteria in bulk water: E. Schwegler, G. Galli, F. Gygi, *Phys. Rev. Lett.* **2000**, *84*, 2429–2432.
[44] For an example of the definition of the pair-correlation function, see M. P. Allen, D. J. Tildesley, *Computer Simulation of Liquids*, Clarendon Press, Oxford, **1987**.
[45] C. E. Reynhardt, *Acta Cryst. Sect. B* **1972**, *28*, 524–529.
[46] For example, 1.899 Å in $K_2(NMe_4)[Co(CN)_6]\cdot 3H_2O$: R. G. Romero, A. D. Morales, J. D. Rodriguez, J. F. Bertran, *Trans. Annu. Meet. Orthop. Res. Soc. Transition Met. Chem.* **1992**, *17*, 573.
[47] The most promising route would probably be a supermolecular approach involving PCM calculations for an explicitly hydrated cluster; however, any single, static equilibrium structure of such a model would be highly arbitrary, and ultimately, one would have to form ensemble averages, as for instance in a recent combined CPMD and PCM study of acetone in water: O. Crescenzi, M. Pavone, P. De Angelis, V. Barone, *J. Phys. Chem. B* **2005**, *109*, 445–453.
[48] It should be kept in mind that both approaches—quantum-mechanical zero-point corrections and MD-based thermal averaging—describe very different things and that it is not possible to simply use the computed changes in r or δ as increments and add them up. However, since both effects have the same physical origin, namely, the anharmonicity of the PES and the curvature of the magnetic shielding hypersurface, it is sensible to discuss them together.
[49] This trend is consistent with the observation that the ^{59}Co nucleus in **1** is shielded with increasing pressure (by ca. 80 ppm at 5 kbar): D. G. Gillies, L. H. Sutcliffe, A. Williams, *J. Magn. Reson.* **2002**, *40*, 57–64.
[50] C. J. Jameson, D. Rehder, M. Hoch, *J. Am. Chem. Soc.* **1987**, *109*, 2589–2594.
[51] An even more deshielded complex containing two tripod ligands with O donors is known, which at ambient temperature shows evidence for significant spin crossover (i.e., thermal population of a paramagnetic high-spin state): G. Navon, W. Kläui, *Inorg. Chem.* **1984**, *23*, 2722–2725.
[52] a) M. E. Tuckerman, K. Laasonen, M. Sprik, M. Parrinello, *J. Chem. Phys.* **1995**, *103*, 150–161; b) D. Marx, M. E. Tuckerman, J. Hutter, M. Parrinello, *Nature* **1999**, *397*, 601–604.
[53] Likewise, no proton transfers were reported in a QM/MM study (at the Hartree–Fock level) for the high-spin state of **2** in water: C. Kritayakornupong, K. Plankensteiner, B. M. Rode, *J. Chem. Phys.* **2003**, *119*, 6068–6072.
[54] We have not included counterions in our simulations, because those present in the experiments (alkali metal cations for **1** and **4**, and halide anions for **2** and **3**) are usually well hydrated, forming solvent-separated, rather than contact ion pairs. Realistic computational modeling of the real solutions would require much larger boxes (or QM parts) and, in particular, much larger simulation times, as the relative diffusion of hydrated ions happens on a longer timescale. It is possible that even such distant counterions could exert noticeable effects on the properties under scrutiny, but most likely this would just fine-tune the latter, not radically alter them.
[55] G. Navon, *J. Chem. Phys.* **1981**, *85*, 3547–3549.
[56] From a) K. B. Yatsimirskii, V. P. Vasil′ev, *Instability Constants of Complex Compounds*, Pergamon Press, Elmsford, New York, **1960**; as cited in b) J. E. Huheey, *Inorganic Chemistry: Principles of Structure and Reactivity*, 3rd ed., Harper & Row Publishers, New York, **1983**.
[57] Review: G. W. Neilson, P. E. Mason, S. Ramos, D. Sullivan, *Philos. Trans. R. Soc. London Ser. A* **2001**, *359*, 1575–1591.
[58] J. K. Beattie, S. P. Best, B. W. Skelton, A. H. White, *J. Chem. Soc. Dalton Trans.* **1981**, 2105–2111.
[59] J. K. Beattie, S. P. Best, *Coord. Chem. Rev.* **1997**, *166*, 391–415.
[60] The actual sensitivity of the magnetic shielding constant for **2** toward r(CoO) is even higher, since the δ values incorporate the geometry dependence of the standard to some extent; the correlation between the raw σ data and r affords a slope of -1001 ppm pm^{-1}.
[61] Deprotonation of an oxygen donor in Co^{III} ammine complexes can also have a pronounced effect on ^{1}H chemical shifts elsewhere in

the complex: K. Hegetschweiler, D. Kuppert, J. Huppert, M. Straka, M. Kaupp, *J. Am. Chem. Soc.* **2004**, *126*, 6728–6738.
[62] For example, a) $[Co(NH_3)_6][Gd(L)_2(H_2O)]\cdot 8H_2O$ (L = nitrilotriacetate): M. S. Maldwin, M. E. Kastner, *Acta Crystallogr. Sect. C* **2002**, *58*, m611–m612; b) $[Co(NH_3)_6][C_6H_3(CH_3SO_3)]_3\cdot 3H_2O$: S. A. Dalrymple, M. Parvez, G. K. H. Shimizu, *Inorg. Chem.* **2002**, *41*, 6986–6996; c) cf. r(Co–N) = 1.957(9)–1.974(6) Å (av 1.963 Å) in $[Co(NH_3)_6]Cl_3$: G. J. Kruger, E. C. Reynhardt, *Acta Crystallogr. Sect. B* **1978**, *34*, 915–917.
[63] At no point is proton transfer from an ammine ligand to the solvent observed.
[64] A referee suggested that the apparent discrepancy between the two approaches could originate from the inherent differences in the QM methods (Gaussian all-electron basis versus plane waves with pseudopotentials). Given the good mutual accord between the CPMD and BOMD results for the pristine complexes, this suggestion appears quite unlikely.
[65] Such an approach has been used, for instance, in ref. [53] and in C. F. Schwenk, H. H. Loeffler, B. M. Rode, *J. Am. Chem. Soc.* **2003**, *125*, 1618–1624.
[66] Unfortunately, this possibility is not yet implemented in the ChemShell program package that we used.
[67] Other force fields and QM/MM coupling schemes could also be tested, for instance, as realized in an interface with CPMD: A. Laio, J. VandeVondele, U. Röthlisberger, *J. Chem. Phys.* **2002**, *116*, 6941–6947.
[68] A similar value of $-381\ ppm\,pm^{-1}$ is obtained from a correlation between r and the raw σ data of **3**.
[69] a) M. R. Bendall, D. M. Doddrell, *Aust. J. Chem.* **1978**, *31*, 1141–1143; b) J. G. Russel, R. G. Bryant, *Anal. Chim. Acta* **1983**, *151*, 227–229; c) J. G. Russel, R. G. Bryant, M. M. Kreevoy, *Inorg. Chem.* **1984**, *23*, 4565–4567.
[70] The concomitant effect of using D_2O instead of H_2O as solvent is much smaller; for example, switching from the latter to the former affects $\delta(^{59}Co)$ of **1** by just 1 ppm: P. Laszlo, A. Stockis, *J. Am. Chem. Soc.* **1980**, *102*, 7818–7820.
[71] F. Asaro, L. Liguori, G. Pellizer, *Angew. Chem.* **2000**, *112*, 2008–2010; *Angew. Chem. Int. Ed.* **2000**, *39*, 1932–1934.
[72] a) For example, mean value 1.759 Å in $[MoCp(CO)_2(PBu_4)_2][Co(CO)_4]\cdot C_6H_5CH_3$: X. Song, T. L. Brown, *Organometallics* **1995**, *14*, 1478–1488. b) For comparison, 1.749 Å in $Na[Co(CO)_4]$: P. Klufers, *Z. Kristallogr.* **1984**, *167*, 275–286.
[73] The apparent shallow maximum in the $g(r)$ curve in Figure 5 around $r \approx 3.5$ Å arises because for distances beyond that value a considerable fraction of the corresponding sphere around the carbonyl O atom is taken up by the complex and cannot be occupied by water molecules from the solvent. As r approaches half the box length, $g(r)$ attains the value of 1 for the ideal random distribution.
[74] See, for instance: N. Juranić, *Coord. Chem. Rev.* **1989**, *96*, 253–290.
[75] For pictorial rationalizations of such paramagnetic contributions see, for instance, refs. [3, 10a] and Y. Ruiz-Morales, T. Ziegler, *J. Phys. Chem. A* **1998**, *102*, 3970–3976.
[76] For recent analyses of transition metal NMR parameters in terms of individual MO pair contributions see, for example: a) L. Orian, A. Bisello, S. Santi, A. Ceccon, G. Saielli, *Chem. Eur. J.* **2004**, *10*, 4029–4040; b) B. Le Guennic, K. Matsumoto, J. Autschbach, *Magn. Reson. Chem.* **2004**, *42*, S99-S116.
[77] M. Bühl, F. T. Mauschick, *Magn. Reson. Chem.* **2004**, *42*, 737–744.

Received: March 14, 2005
Published online: September 30, 2005

